
Breaking the Chain of Gradient Leakage in Vision Transformers

Yahui Liu^{*†}
University of Trento
yahui.liu@unitn.it

Bin Ren[†]
University of Trento
bin.ren@unitn.it

Yue Song
University of Trento
yue.song@unitn.it

Wei Bi
Tencent AI Lab
victoriabi@tencent.com

Nicu Sebe
University of Trento
niculae.sebe@unitn.it

Wei Wang
University of Trento
wei.wang@unitn.it

Abstract

User privacy is of great concern in Federated Learning, while Vision Transformers (ViTs) have been revealed to be vulnerable to gradient-based inversion attacks. We show that the learned low-dimensional spatial prior in position embeddings (PEs) accelerates the training of ViTs. As a side effect, it makes the ViTs tend to be position sensitive and at high risk of privacy leakage. We observe that enhancing the *position-insensitive* property of a ViT model is a promising way to protect data privacy against these gradient attacks. However, simply removing the PEs may not only harm the convergence and accuracy of ViTs but also places the model at more severe privacy risk. To deal with the aforementioned contradiction, we propose a simple yet efficient Masked Jigsaw Puzzle (MJP) method to break the chain of gradient leakage in ViTs. MJP can be easily plugged into existing ViTs and their derived variants. Extensive experiments demonstrate that our proposed MJP method not only boosts the performance on large-scale datasets (*i.e.*, ImageNet-1K), but can also improve the privacy preservation capacity in the typical gradient attacks by a large margin. Our code is available at: <https://github.com/yh1leo/MJP>.

1 Introduction

Federated learning (FL) [32, 45] has recently emerged as a new collaborative and distributed learning paradigm, and its primary goal is to share weight updates or gradients during training to protect user-level privacy and data access rights [50]. Therefore, the key privacy concern for users is whether model updates reveal too much about the data when they are attacked by gradient inversion methods. A strong defense against these attacks is aggregation, *e.g.*, the user only reports model updates aggregated over a significant number of local data points [5]. However, recent attack methods reveal that it is still feasible to recover the user data from the aggregated gradients [60, 19].

In general, the fundamental principle of these attacks is that each sample activates only a portion of content-related neurons in the deep neural networks, leading to different backward gradients for different samples. This empirical observation raises an immediate question: *Can users apply transformed data instead of the original data into a transformation-invariant model during the training?* Such strategy and model allow the different variants of the same original data to have the same (or similar) backward gradients, which may intuitively alleviate the privacy preservation issue.

^{*}Work done as intern at the Tencent AI Lab.

[†]Equal contributions.

The recently emerged Vision Transformers (ViTs) [14] are potential options for building such transformation-invariant models. As a core module in ViTs, multi-head self-attentions (MSAs) [49, 14] aggregate sequential tokens with normalized attentions as:

$$z_j = \sum_i \text{Softmax}\left(\frac{QK}{\sqrt{d}}\right)_i V_{i,j} \quad (1)$$

where Q , K and V are query, key and value matrices, respectively. d is the dimension of query and key, and z_j is the j -th output token. In theory, the outputs of MSAs should be entirely invariant to the input sequence order (*i.e.*, *position-insensitive*). This indicates a promising direction to transform a visually recognizable image into its unrecognizable counterpart while maintaining the performance compared with training on the original data. However, the usage of position embeddings hinders such implementations, where the outputs of the ViTs can dramatically vary a lot with the mentioned transformations. Moreover, the recent work [38] reveals that jointly using MSAs and learnable position embeddings places the model at severe privacy risk. All of these indicate that position embeddings could be a key to solve gradient leakage in ViTs.

In this paper, we first propose that translating visually recognizable image into its unrecognizable counterpart is feasible to train ViTs at a comparable (or even better) performance with the state-of-the-art (SOTA). Especially, such transformation (*e.g.*, randomly shuffling patches) significantly increases the difficulty of recovering the user-level data through the aggregated gradients. However, the aforementioned transformation can degenerate the positive effects of position embeddings in ViTs. As a remedy, we can transform a portion of the sequence patches. In this scenario, once we maintain the original sequence of position embeddings, it leads to a mismatching issue between the shuffled patches and the sequential position embeddings. Therefore, we introduce a shared *unknown* position embedding instead to alleviate the mismatching issue for the shuffled patches. Moreover, we revisit the remaining position embeddings (*i.e.*, corresponding to the non selected patches) and discover that applying a low-dimensional prior on them (*e.g.*, Principal Component Analysis (PCA) or MLP projecting to 2D space) is helpful for integrating the spatial information to these position embeddings, leading to performance gains.

According to these observations, we propose a Masked Jigsaw Puzzle (MJP) method to break the chain of gradient leakage in ViTs from a new perspective. There are four core procedures in the proposed MJP method: (1) We first utilize a block-wise masking method [2] to randomly select a part of the input sequential patches; (2) Then, we apply jigsaw puzzle to the selected patches (*i.e.*, shuffles the orders); (3) After that, we introduce a shared *unknown* position embedding for the shuffled patches instead of using the original position embeddings. (4) To well maintain the position prior, we introduce a *dense absolute localization* (DAL) regression to the position embeddings of the unmasked patches in a self-supervised manner.

In summary, our main contributions are:

1. To our best knowledge, we are the first to solve the gradient leakage in ViTs by revisiting the effects of position embeddings and enhancing the position-insensitive property of ViTs. Especially, we introduce a simple yet efficient MJP method can be easily plugged into the existing ViTs, which pilots the new direction for exploring the position embeddings.
2. Extensive experimental results show that our proposed method can not only alleviate the gradient leakage problem in ViTs, but also boosts the accuracy and robustness on large-scale datasets (*e.g.*, ImageNet-1K [43] and ImageNet-C [23], -A/O [24]).

2 Related Work

Position Embeddings. Transformers [49], originally designed for Nature Language Processing (NLP) tasks, have recently shown promising performance for computer vision tasks [18, 29]. Benefiting from the larger representation capacity of capturing global relations between image elements, Vision Transformers (ViTs) [14] have achieved superior performance than their counterpart CNNs for image classification and various downstream tasks (*e.g.*, object detection [6, 69], object re-identification [22], dense prediction [59, 66, 55, 53] and image generation [10, 9, 33, 27]).

Notably, position embeddings are usually applied to alleviate the lack of inductive bias in ViTs. For example, previous works [16, 49, 44] indicated that position embeddings are useful to give the

model a sense of which portion of the sequence in the input or output it is currently dealing with. Inspired by this, some works [28, 46, 31, 35, 20] showed complex application scenarios benefit from the usage of suitable position embeddings. For example, Chu *et al.* [11] proposed correlating the position embeddings with their local neighborhood of the input sequence. Liu *et al.* [34] proposed to enhance the spatial prior (*i.e.*, relative localization) in the final content embedding to indirectly enrich the inductive bias. Obviously, although these methods enhance the position information learnt by position embeddings, they indeed degenerate the position-insensitive property of MSAs.

Especially, Wang *et al.* [54] revealed that Transformer encoders (*e.g.*, BERT [13] and RoBERTa [36]) may not well capture the meaning of positions (absolute and relative positions). They showed that Transformer encoders learn the local position information that can only be effective in masked language modeling. In contrast, it does not exist such a similar “masked language modeling” procedure in ViTs (and VTs) in the typical supervised pre-training. Moreover, Lu *et al.* [38] revealed that the learnable position embeddings place the model at severe privacy risk, which leaks the clues of reconstructing sequential patches to images. In this paper, we dive into the usage of position embeddings and propose an efficient method to alleviate the gradient leakage issue in ViTs.

Privacy-Preserving Learning. The original intention of the federated or collaborative learning is to prevent the direct privacy leakage via making the sensitive data invisible to collaborators [3, 12, 68]. Various strategies, including gradient aggregation, gradient compression [51, 8] and gradient encryption [4, 1], were applied to reduce the privacy leakage. Recently, several works showed that the private training data can be recovered via elaborately designed attack methods from the shared parameters and the corresponding gradients. For example, analytic attacks [41, 1, 15] utilized a learnable affine function that can be directly computed from the gradient. However, analytic recovery of this kind only succeeds for a single data point. Recursive attacks [67, 40] extended analytic attacks to models with more than only linear layers to recover only the average of input images.

Meanwhile, optimization-based attacks [56, 68, 65, 52, 26, 42, 19] tried to solve it as a gradient matching problem showing promising results on both NLP and computer vision tasks. For example, Zhu *et al.* [68] showed that it is challenging to recover the private data based on the leaked gradients for the cases in which the batch size is large or the training input is at the high resolution. However, this assumption was only verified with a very shallow attack network. After that, some methods [60, 17, 61] demonstrated that it was feasible to attack even the deep CNN models like ResNet-50 [21] with large input batch size by designing elaborate strategies.

Among these methods, GradInversion [60] demonstrated the first successful scaling of gradient inversion to deep CNNs on large-scale datasets (*e.g.*, ImageNet-1K) over large batches. They formulated an optimization task that converts random noises into natural images, matching gradients while regularizing image fidelity. APRIL [38] analysed the gradient leakage risk of self-attention based models like ViTs. Especially, they revealed that the position embeddings not only encode positional information for patches but also enables gradient leakage from the layer. Then, GradViT [19] also demonstrated that ViTs suffer even more data leakage compared to CNNs. With tailored scheduler and constraints, they can achieve a valid image recovery. These methods indicate the fact that both CNNs and ViTs can be attacked from the updated gradients with proper strategies in federated learning. Fortunately, we find some clues for alleviating the gradient leakage issue in ViTs from previous work, where the remedy may be hidden behind understanding the position embeddings.

3 Preliminaries

3.1 Explicitly Enforcing Position Embeddings Low-dimensional Spatial Priors

Although numerous works claim that the positional embedding can learn the 2-D spatial relationship of image patches, this point has not been demonstrated visually or mathematically. To visualize the concrete relation of image patches, we project the high-dimensional position embedding into the 2-D and 3-D spaces using Uniform Manifold Approximation and Projection (UMAP) [39] and PCA, respectively. Figure 1 displays the projections of position embeddings from DeiT-S [48]. For the UMAP, the projected positional embedding emerges as grid-like structures with the distances between each point roughly the same, which is coherent to the relation of embedded image patches. For the PCA, the position embedding that corresponds to neighboring image patches groups together and aggregates to the stick-like form. This phenomenon demonstrates that the spatial relationship is

indeed learned by the positional embeddings. Moreover, this also implies that *the spatial relationship learned in the high-dimensional space still manifests in the low-dimensional space.*

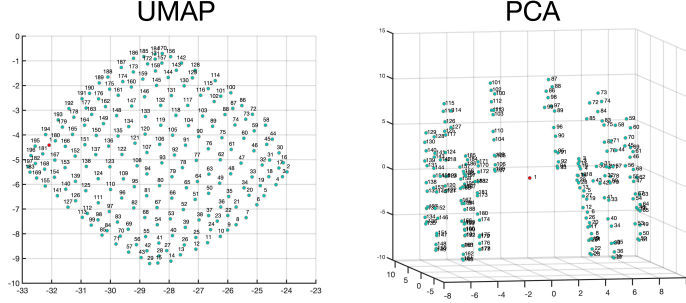


Figure 1: Low-dimensional projection of position embeddings from DeiT-S [48]. The embedding of index 1 (*highlighted in red*) corresponds to the [CLS] embedding that does not embed any positional information.

The learnable positional embedding, which works as a lookup table of a dictionary, maps the 1-dimensional data into the sparse high-dimensional space. By nature, it is a sparse large matrix. Dimensionality reduction techniques can capture the structural information of a sparse matrix using a low dimensionality. For the PCA, the amount of information retained in the projection can be measured by the ratio of explained variance. Formally, we have the definition as follows:

Definition 1 (Explained Variance) *Let \mathbf{P} and \mathbf{V} denote the data matrix and the PCA projection matrix, respectively. The ratio of explained variance that $\mathbf{P}\mathbf{V}$ accounts for is defined as $\sum \sigma(\mathbf{P}\mathbf{V})^2 / \sum \sigma(\mathbf{P})^2$ where $\sigma(\cdot)$ denotes the singular value.*

In practice, we observe that the 3-dimensional PCA projection explains 54.6% of the total variance of the DeiT-S embedding matrix. Given that a large amount of information can be captured by the low-dimensional projection, we propose that explicitly enforcing low-dimensional positional prior can help the positional learning in the high-dimensional space, which might accelerate the convergence of training and improve the performance (See Section §4.1).

3.2 Improving Privacy Protection against Gradient Leakage by Random Patch Permutation

Existing analytic gradient attack algorithms mainly model the problem as a linear system with closed-form solutions [67, 38]. For ViTs, the linear system is defined as:

$$\frac{\partial l}{\partial \mathbf{z}_0} \mathbf{z}_0^T = \mathbf{Q}^T \frac{\partial l}{\partial \mathbf{Q}} + \mathbf{K}^T \frac{\partial l}{\partial \mathbf{K}} + \mathbf{V}^T \frac{\partial l}{\partial \mathbf{V}} \quad (2)$$

where \mathbf{z}_0 denotes the image embedding that consists of patch embedding and positional embedding (i.e., $\mathbf{z}_0 = \mathbf{x}_p \mathbf{E} + \mathbf{E}_{\text{pos}}$, where \mathbf{x}_p denotes the sequence of flattened 2D patches and \mathbf{E} represents the trainable linear projection). Since we have $\partial l / \partial \mathbf{z} = \partial l / \partial \mathbf{E}_{\text{pos}}$, the positional embedding layer is thus vulnerable to the gradient leakage attack. When the gradient $\partial l / \partial \mathbf{E}_{\text{pos}}$ is accessible, the image can be reconstructed as:

$$\mathbf{x}_p = \left(\left(\frac{\partial l}{\partial \mathbf{E}_{\text{pos}}} \right)^{-1} \left(\mathbf{Q}^T \frac{\partial l}{\partial \mathbf{Q}} + \mathbf{K}^T \frac{\partial l}{\partial \mathbf{K}} + \mathbf{V}^T \frac{\partial l}{\partial \mathbf{V}} \right) - \mathbf{E}_{\text{pos}} \right) \mathbf{E}^{-1} \quad (3)$$

As indicated above, the gradient leakage of the positional embedding layer can make the image easily reconstructed with closed-form solutions. To resolve this issue, we propose to randomly permute a portion of the image patches (See Section §4.2). The random permutation will drastically change both \mathbf{E}_{pos} and $\partial l / \partial \mathbf{E}_{\text{pos}}$ in the above equation. This could significantly increase the difficulties to solve the linear system and reconstruct the image. Notice that for the optimization-based attack [68], the patch permutation would also greatly affect the objective $\min \|\nabla \mathbf{x}_p - \nabla \tilde{\mathbf{x}}_p\|^2$ where $\tilde{\mathbf{x}}_p$ denotes the transformed patch sequence.

4 Method

In this section, we first introduce the low-dimensional sparse prior to guide the position information in the learnable position embeddings. Then, we show details on the proposed Masked Jigsaw Puzzle (MJP) method.

4.1 Aggregating Spatial Prior in Position Embeddings

Liu *et al.* [34] noticed that the gains of accelerating training convergence result from enhancing the 2-D spatial information in the output embeddings of the last layer. Inspired by their work, we observe that such gains can also be directly obtained by applying a low-dimensional spatial prior in position embeddings. Different from their dense relative localization constraint, we propose a simpler *dense absolute localization* (DAL) regression, which can get rid of sampling relative pairs.

Once a position embedding can actually capture its absolute position, to some extent, such position information could be reconstructed by a reversed mapping function $g : \mathcal{E} \rightarrow \mathcal{P}$, where \mathcal{E} and \mathcal{P} are embedding space and position space, respectively. Given position embeddings correspond to the sequential image patches, we can reshape them into $\mathbf{E}_{\text{pos}} \in \mathbb{R}^{K \times K \times D}$, where K refers to height/weight of the grid and D refers to latent vector size. Let $(\tilde{i}, \tilde{j})^T = g(\mathbf{E}_{\text{pos}}^{i,j})$, we can calculate the DAL loss as:

$$\mathcal{L}_{\text{DAL}} = \mathbb{E}_{\mathbf{E}_{\text{pos}}^{i,j}, 1 \leq i, j \leq K} [\| (i, j)^T - (\tilde{i}, \tilde{j})^T \|_1], \quad (4)$$

where the expectation is computed by averaging the ℓ_1 loss between the correspond $(i, j)^T$ and $(\tilde{i}, \tilde{j})^T$. Then, \mathcal{L}_{DAL} is added to the standard cross-entropy loss (\mathcal{L}_{CE}) of the native ViTs. The final loss is: $\mathcal{L}_{\text{all}} = \mathcal{L}_{\text{CE}} + \lambda \mathcal{L}_{\text{DAL}}$, where we set $\lambda = 0.01$ for all experiments. Note that the mapping function can be either linear or nonlinear. Throughout this work, we mainly discuss three implementations, including non-parametric PCA, learnable linear (LN), and nonlinear (NLN) projection layers.

4.2 Masked Jigsaw Puzzle

The goal of MJP is to enhance the capacity of position insensitivity that directly increases the difficulties of image recovery from gradient updates, while to preserve the accuracy on the standard classification in the pre-training. In practice, image masking methods are commonly applied in recent vision task [2, 57, 20, 58, 7], which is a useful and off-the-shelf strategy for self-supervised image reconstruction. Given an input image $\mathbf{x} \in \mathbb{R}^{H \times W \times C}$, we reshape it into a sequence of flattened 2D patches $\mathbf{x}_p \in \mathbb{R}^{N \times (P^2 \cdot C)}$, where (H, W) is the resolution of the original image, C is the number of channels, (P, P) is the resolution of each image patch, and $N = HW/P^2$ is the resulting number of patches. Usually, we can formulate the input layer before feeding the sequential features into the Transformer block as follows:

$$\mathbf{z}_0 = [\mathbf{x}_{\text{CLS}}; \mathbf{x}_p^1 \mathbf{E}; \mathbf{x}_p^2 \mathbf{E}, \dots, \mathbf{x}_p^N \mathbf{E}] + \mathbf{E}_{\text{pos}}, \quad (5)$$

where $\mathbf{E} \in \mathbb{R}^{(P^2 \cdot C) \times D}$ is a trainable linear projection layer and refer to the output of linear projection as the patch embeddings, and $\mathbf{E}_{\text{pos}} \in \mathbb{R}^{(N+1) \times D}$ refers to position embeddings (the additional one is applied to the [CLS] embedding).

Then, we assign a binary mask matrix $\mathbf{m} \in \mathbb{R}^{\frac{H}{P} \times \frac{W}{P}}$ corresponding to the patches in \mathbf{x}_p . We apply the block-wise masking strategy [2] on the mask matrix \mathbf{m} , where the masked positions are set to 1 and the left positions are set to 0, the hyper-parameter $\gamma = \sum_i \mathbf{m}_i / N$ is used to control the ratio of selected positions. After that, we apply jigsaw-puzzle shuffling to the selected patches in \mathbf{x}_p , where the selected patches are the set $\{\mathbf{x}_p^i | \mathbf{m}_i = 1\}$. Therefore, we refer $\tilde{\mathbf{x}}_p$ to the shuffled patch sequence. With the mask matrix \mathbf{m} , we can update the position embeddings in this manner:

$$\tilde{\mathbf{E}}_{\text{pos}}^i = \begin{cases} \mathbf{E}_{\text{pos}}^i, & \text{if } \mathbf{m}_i = 0; \\ \mathbf{E}_{\text{unk}}, & \text{if } \mathbf{m}_i = 1, \end{cases} \quad (6)$$

where $\mathbf{E}_{\text{unk}} \in \mathbb{R}^{1 \times D}$ refers to a share learnable embedding (*i.e.*, *unknown* position embedding) to represent that the image patch in this position is randomly permuted. Thus, we replace the input layer with a new formulation:

$$\tilde{\mathbf{z}}_0 = [\mathbf{x}_{\text{CLS}}; \tilde{\mathbf{x}}_p^1 \mathbf{E}; \tilde{\mathbf{x}}_p^2 \mathbf{E}, \dots, \tilde{\mathbf{x}}_p^N \mathbf{E}] + \tilde{\mathbf{E}}_{\text{pos}}. \quad (7)$$

Then, the following procedures and modules are exactly what they are in the original ViTs. Obviously, the MJP method can be also regarded as a data augmentation method, where it feeds images with randomly shuffled patches to ViTs. On the one hand, it not only boosts the accuracy on the standard classification in the pre-training but also improves the position-insensitive property of ViTs. On the other hand, given that the block-wise sampling and shuffling in the proposed MJP are non-differentiable, it intuitively can increase the difficulties in directly recovering the original images with gradient updates (See Section §5.2).

5 Experiments

5.1 Supervised Pre-training

We first follow the typical supervised pre-training procedure, where all the compared models are trained on ImageNet-1K to show the capacity of our proposed MJP method.

Setting. For image classification, we benchmark the proposed MJP method on ImageNet-1K [43], which contains 1.28M training images and 50K validation images from 1,000 classes. The training details mostly follow the training protocols³ from Touvron *et al.* [48].

Table 1: Comparisons of different backbones on ImageNet-1K classification.

| Method | Img Size | Param. | Top-1 Acc. ↑ | Diff. Norm. ↓ | Consistency ↑ |
|-----------------|----------|--------|--------------|---------------|---------------|
| ResNet-50 [21] | 224 | 25 | 79.3 | 11.77 | 51.5 |
| ResNet-50 + MJP | 224 | 25 | 79.4 | 7.11 | 69.3 |
| DeiT-S [48] | 224 | 22 | 79.8 | 16.21 | 64.3 |
| DeiT-S + MJP | 224 | 22 | 80.5 | 8.96 | 82.9 |
| Swin-T [37] | 224 | 29 | 81.3 | 15.49 | 41.5 |
| Swin-T + MJP | 224 | 29 | 81.3 | 12.36 | 66.9 |

Results with regular ImageNet-1K training. We mainly compare with four typical existing methods, including two state-of-the-art Visual Transformers (*i.e.*, DeiT [48] and Swin [37]) and one widely-used CNN-based ResNet-50 [21]. All these methods are with comparable size (*i.e.*, less than 30M parameters). Besides the common Top-1 accuracy (**Top-1 Acc.**), we also report another two evaluation metrics to show the robustness of a model on the jigsaw puzzle transformation. For a given input image \mathbf{x} , we collect its counterpart $\tilde{\mathbf{x}}$ by applying masked jigsaw puzzle to shuffle a portion of selected patches. Then, we calculate the difference ℓ_2 -norm (*i.e.*, **Diff. Norm.**) between the [CLS] embedding inferred from \mathbf{x} and $\tilde{\mathbf{x}}$: $\|\mathcal{F}_{\text{CLS}}(\mathbf{x}) - \mathcal{F}_{\text{CLS}}(\tilde{\mathbf{x}})\|_2^2$. For **Consistency**, we check how often a model outputs the same classification, given the \mathbf{x} and $\tilde{\mathbf{x}}$: $\mathbb{E}_{\mathbf{x}}[\mathbb{1}\{\arg \max P(\mathcal{F}(\mathbf{x})) = \arg \max P(\mathcal{F}(\tilde{\mathbf{x}}))\}]$. For a fair comparison, we use $\gamma = 0.5$ (*i.e.*, half of the total patches are shuffled) to create $\tilde{\mathbf{x}}$ in Table 1. According to these results, our proposed MJP method can not only boost the classification accuracy but also significantly improves Diff. Norm. and Consistency. Moreover, MJP works well in the variants of ViTs (*e.g.*, Swin), which shows a good potential capacity of generalization.

Discussion on Variants of MJP. We test several variants of the proposed MJP, including (1) Removing the position embeddings (PEs) from the original DeiT-S; (2) SPP: shuffling both the 16×16 patches and pixels within the patches, which is tested in MLP-Mixer [47] to validate the invariance to input permutations; (3) JP: applying masked jigsaw puzzle to the sequence patches; (4) IDX: using an additional collect of embeddings to indicate the global indexes for the input patches; (5) UNK: replacing the position embeddings in the masked positions with a shared *unknown position embedding*; (6) DAL: jointly learning *dense absolute localization* regression in a self-supervised manner during the pretraining, where we provide PCA, linear (LN) and nonlinear (NLN) projections, respectively.

Table 2 shows the detailed ablation study on the variants of our proposed MJP method. First, as we expect, when we remove the position embeddings from the original DeiT-S model, the accuracy obviously decreases (*i.e.*, -2.3%) but the consistency achieves 100%. It verifies that that the ViTs are naturally position-insensitive once without using position embeddings. We observe that the previous SPP strategy harms the accuracy of the model (*i.e.*, -4.9%), which indicates it is not sufficient to

³<https://github.com/facebookresearch/deit>

simply shuffle both patches and pixels in the input image. As we expect, the usage of UNK embedding alleviates the confusion between shuffled and unshuffled positions, which boosts both the accuracy and consistency performances. Finally, we can find that using *dense absolute localization* regression on the unmasked position embeddings can marginally boost the accuracy. Although PCA does not involve more parameters to the model, it significantly increases the computation latency (e.g., +46% with only 5 iterations). In general, it is better to use a nonlinear projection (e.g., a 3-layers MLP with negligible computation latency) to allow the learned position embeddings aggregating more additional information.

Table 2: Ablation study on the variants of the proposed MJP method.

| Method | Top-1 Acc. \uparrow | Consistency \uparrow |
|-----------------------------|-----------------------|------------------------|
| A: DeiT [48] | 79.8 | 64.3 |
| B: A - PEs | 77.5 (-2.3) | 100.0 |
| C: A + SPP [47] | 74.9 (-4.9) | 74.8 |
| D: A + DAL (NLN) | 80.0 (+0.2) | 64.0 |
| E: A + JP | 79.2 (-0.6) | 73.8 |
| F: A + JP + IDX | 79.9 (+0.1) | 79.6 |
| G: A + JP + UNK | 80.1 (+0.3) | 83.8 |
| H: A + JP + UNK + DAL (PCA) | 79.9 (+0.1) | 83.4 |
| I: A + JP + UNK + DAL (LN) | 80.0 (+0.2) | 83.8 |
| J: A + JP + UNK + DAL (NLN) | 80.5 (+0.7) | 82.9 |

Table 3: Ablation study on the proposed MJP method trained with different masking ratio γ .

| Metric | Masking Ratio | | | | | |
|-------------|---------------|------|------|------|------|------|
| | 0 | 0.1 | 0.3 | 0.5 | 0.7 | 0.9 |
| Top-1 Acc. | 80.0 | 80.5 | 80.3 | 80.4 | 80.2 | 80.3 |
| Diff. Norm. | 16.56 | 8.96 | 6.36 | 5.23 | 4.39 | 3.97 |
| Consistency | 64.0 | 82.9 | 88.1 | 90.5 | 92.3 | 93.1 |

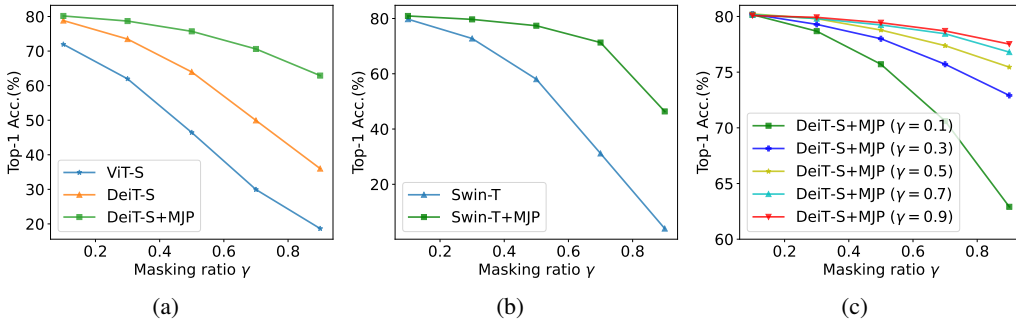


Figure 2: Ablation on the masking ratio γ during the inference: (a) comparisons among ViT-S, DeiT-S and our method (trained with $\gamma = 0.1$); (b) comparisons between Swin-T and our method (trained with $\gamma = 0.1$); (c) comparisons of our proposed method on DeiT-S trained with different γ .

Results with different Jigsaw Puzzle ratios. As shown in Table 3, we test different masking ratios used in the block-wise masking strategy during the training. Obviously, Diff. Norm. is with inverse tendencies compared to Consistency, where a smaller Diff. Norm. score usually indicates a larger (better) consistency score. Comparing the accuracy trained with $\gamma > 0$, it shows our model is not sensitive to different γ . In particular, a small masking ratio (e.g., $\gamma = 0.1$) is sufficient for boosting the accuracy. In addition, a large masking ratio can significantly reduce the Diff. Norm. and improve the consistency.

For a model trained with a fixed γ , we also test accuracy with different masking ratios during the inference. As shown in Figure 2 (a) and (b), the performances of original models drop significantly

when we shuffle more image patches. In contrast, our proposed method shows more consistent performances in the same scenarios. Moreover, the model trained a larger γ is inclined to be more consistent as shown in Figure 2 (c).

Informativeness of the position embeddings. For a position space \mathcal{P} (*i.e.*, a 1-dim or 2-dim space), we may not need a high-dimension embedding space \mathcal{X} to model the positions. To measure the informativeness of the learned position embeddings, we apply singular value decomposition (SVD) to position embeddings and analyze their eigenvalue distributions. Figure 3 plots the curves of accumulated top- n eigenvalues versus the proportion of total eigenvalues. Once the most proportion of total eigenvalues for a position embedding is with only a very small n , it indicates the position embedding may learn more complex information rather than only about positions. Supposing that we are using PCA to project the positional embedding of both matrices, to achieve the same explained variance ratio, our MJP needs more singular values (*i.e.*, large dimensionality) than DeiT-S. This indicates that our positional embedding matrix is more informative. Similar finding is also revealed by Wang *et al.* [54]. Benefiting from the additional information, we show in Section §5.2 that it indeed increases the difficulties of recovering image from gradient updates. In other words, our proposed MJP reduces the risk of gradient leakage from the learned position embeddings.

Robustness on challenging datasets. ImageNet-C [23] benchmarks a classifier’s robustness to common corruptions⁴. The mean Corruption Error (mCE) is used to measure the generalization of a model at corrupted distributions (the lower the better). ImageNet-A/O [24] focus on adversarial examples and enable us to either test image classification performance when the input data distribution shifts (*i.e.*, Acc and AURRA), or test out-of-distribution detection performance when the label distribution shifts (*i.e.*, AUPR)⁵. As shown in Table 4, our proposed MJP method not only boosts the accuracy on the standard evaluation on ImageNet-1K validation set but also obviously improves the robustness on the adversarial samples. We guess that MJP enforces the ViTs aware of both local and global context features, which is helpful for getting rid of some sample-specific local features during the training. This is partly verified by the visualization maps in Figure 4, where the last self-attention of our proposed method presents more diverse and content-aware attentions than original DeiT-S.

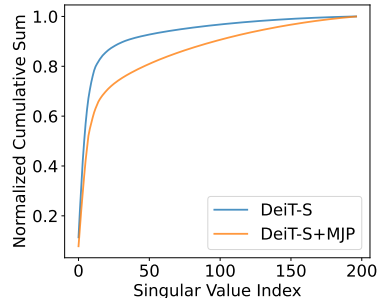


Figure 3: Accumulated top eigenvalues of position embeddings between DeiT-S and our method.

Table 4: Comparisons on robustness to common corruptions and adversarial examples.

| Method | ImageNet-C | ImageNet-A | | ImageNet-O |
|--------------|-------------|-------------|-------------|-------------|
| | mCE ↓ | Acc ↑ | AURRA ↑ | AUPR ↑ |
| DeiT-S | 44.0 | 19.2 | 25.1 | 20.9 |
| DeiT-S + MJP | 41.5 | 21.6 | 29.8 | 22.6 |

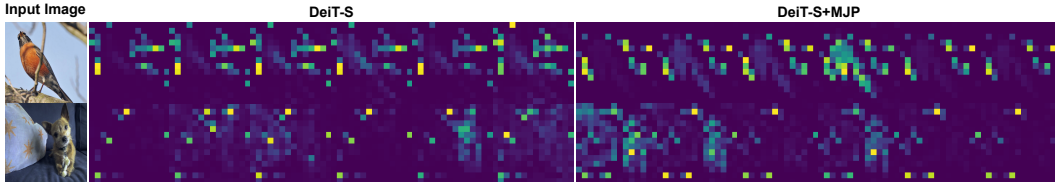


Figure 4: Visual comparisons between visualization maps of the last self-attention in DeiT-S [48] and our proposed DeiT-S+MJP.

⁴<https://github.com/hendrycks/robustness>

⁵<https://github.com/hendrycks/natural-adv-examples>

5.2 Privacy Preservation

We utilize the public protocols⁶ for recovering image with gradient updates in the privacy attack. In this privacy attack, we apply the Analytic Attack proposed in APRIL [38], which is designed for attacking the ViTs. We randomly sample 1K images from the validation set of ImageNet-1K (*i.e.*, one image per category). To evaluate the anti-attack performance of a model, we introduce image similarity metrics to account for pixel-wise mismatch, including Mean Square Error (MSE), Peak Signal-to-Noise Ratio (PSNR), cosine similarity in the Fourier space (FFT_{2D}), and Learned Perceptual Image Patch Similarity (LPIPS) [64]. Different from the evaluation in gradient attacks [38, 19, 60], a model supposed to be with better capacity of privacy preservation when the recovered images from its gradient updates are less similar to the ground truth images.

Table 5 shows the quantitative comparisons between our method and the original ViTs for batch gradient inversion on ImageNet-1K. APRIL [38] enables a viable, complete recovery of original images from the gradient updates of the original ViTs. However, it performs worse in recovering from “DeiT-S+MJP”, leading to best performances on all evaluation metrics and outperform others by a large margin. More surprisingly, our proposed method makes APRIL yield irrerecognizable images and lose a lot of original details in the original images (*i.e.*, noisy patches in the outputs), as shown in Figure 5. We also notice that DeiT-S without using position embeddings is inclined to be at higher risk of privacy (*i.e.*, easier to be attacked by gradients). These promising results indicate that our proposed MJP method is a strong strategy to protect user privacy in FL.

Table 5: Comparisons on gradient leakage by analytic attack [38] with ImageNet-1K validation set, where we test (a) the standard setting that ViT-S, DeiT-S and our model use the original image as input; (b) ViT-S, DeiT-S and our model use the transformed images (*i.e.*, MJP with $\gamma = 0.9$) as input; (c) ablation on without (w/o) using \mathbf{E}_{unk} with the transformed inputs; and (d) the metrics are calculated between original image and reconstructed image. In (a), (b) and (c), the metrics are conducted between the input image and reconstructed image.

| Model | Setting | Acc. \uparrow | MSE \uparrow | FFT_{2D} \uparrow | PSNR \downarrow | SSIM \downarrow | LPIPS \uparrow |
|-------------------|---------|-----------------|----------------|------------------------------|-------------------|-------------------|------------------|
| ViT-S [14] | (a) | 78.1 | .0278 | .0039 | 19.27 | .5203 | .3623 |
| DeiT-S [48] | | 79.8 | .0350 | .0057 | 18.94 | .5182 | .3767 |
| DeiT-S (w/o PEs) | | 77.5 | .0379 | .0082 | 20.22 | .5912 | .2692 |
| DeiT-S+MJP | | 80.5 | .1055 | .0166 | 11.52 | .4053 | .6545 |
| ViT-S [14] | (b) | 18.7 | .0327 | .0016 | 18.44 | .6065 | .2836 |
| DeiT-S [48] | | 36.0 | .0391 | .0024 | 17.60 | .5991 | .3355 |
| DeiT-S (w/o PEs) | | 77.5 | .0379 | .0025 | 20.25 | .6655 | .2370 |
| DeiT-S+MJP | | 62.9 | .1043 | .0059 | 11.66 | .4493 | .6519 |
| DeiT-S+MJP (w/o) | (c) | 40.6 | .1043 | .0059 | 11.66 | .4493 | .6519 |
| DeiT-S+MJP | (d) | 62.9 | .1706 | .0338 | 8.07 | .0875 | .8945 |

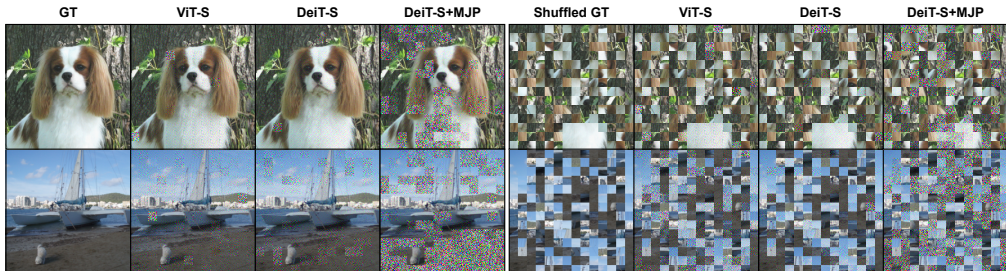


Figure 5: Visual comparisons on image recovery with gradient updates [38]. Our proposed DeiT-S+MJP model significantly outperforms the original ViT-S [14] and DeiT-S [48] models.

⁶<https://github.com/JonasGeiping/breaching>

6 Conclusion

In this paper, we are first to pave the way for investigating position embeddings in the ubiquitous ViTs for the gradient leakage problem. We observe that it is useful to use a sparse spatial prior to directly guide the position embeddings. Then, we propose an easy-to-reproduce yet very effective tool (Masked Jigsaw Puzzle) to significantly alleviate the gradient leakage recovered by gradient attacks while does not degenerate the accuracy on the large-scale dataset (*i.e.*, ImageNet-1K). In a certain sense, the proposed MJP method is also a data augmentation technique, which also boosts the robustness to the common corruptions (*e.g.*, ImageNet-C) and adversarial examples (*e.g.*, ImageNet-A/O). We believe that our method pilots a new direction for privacy preservation during the training.

Limitations We focus on the ViTs with learnable position embeddings in the main experiments. Besides, we notice that some well recovered images patches are with high scores in the attention map, which is a useful clue for better privacy preservation. However, this is out of the scope of this paper. We leave these interesting observations to the future work.

References

- [1] Yoshinori Aono, Takuya Hayashi, Lihua Wang, Shiho Moriai, et al. Privacy-preserving deep learning via additively homomorphic encryption. *IEEE Transactions on Information Forensics and Security*, 13(5):1333–1345, 2017.
- [2] Hangbo Bao, Li Dong, and Furu Wei. Beit: Bert pre-training of image transformers. In *International Conference on Learning Representations (ICLR)*, 2022.
- [3] Keith Bonawitz, Hubert Eichner, Wolfgang Grieskamp, Dzmitry Huba, Alex Ingerman, Vladimir Ivanov, Chloe Kiddon, Jakub Konečný, Stefano Mazzocchi, Brendan McMahan, et al. Towards federated learning at scale: System design. *Proceedings of Machine Learning and Systems*, 1:374–388, 2019.
- [4] Keith Bonawitz, Vladimir Ivanov, Ben Kreuter, Antonio Marcedone, H Brendan McMahan, Sarvar Patel, Daniel Ramage, Aaron Segal, and Karn Seth. Practical secure aggregation for federated learning on user-held data. *arXiv preprint arXiv:1611.04482*, 2016.
- [5] Keith Bonawitz, Vladimir Ivanov, Ben Kreuter, Antonio Marcedone, H Brendan McMahan, Sarvar Patel, Daniel Ramage, Aaron Segal, and Karn Seth. Practical secure aggregation for privacy-preserving machine learning. In *proceedings of the ACM SIGSAC Conference on Computer and Communications Security*, 2017.
- [6] Nicolas Carion, Francisco Massa, Gabriel Synnaeve, Nicolas Usunier, Alexander Kirillov, and Sergey Zagoruyko. End-to-end object detection with transformers. In *European Conference on Computer Vision (ECCV)*, 2020.
- [7] Huiwen Chang, Han Zhang, Lu Jiang, Ce Liu, and William T Freeman. Maskgit: Masked generative image transformer. *arXiv preprint arXiv:2202.04200*, 2022.
- [8] Chia-Yu Chen, Jiamin Ni, Songtao Lu, Xiaodong Cui, Pin-Yu Chen, Xiao Sun, Naigang Wang, Swagath Venkataramani, Vijayalakshmi Viji Srinivasan, Wei Zhang, et al. Scalecom: Scalable sparsified gradient compression for communication-efficient distributed training. In *Advances in Neural Information Processing Systems (NeurIPS)*, 2020.
- [9] Hanting Chen, Yunhe Wang, Tianyu Guo, Chang Xu, Yiping Deng, Zhenhua Liu, Siwei Ma, Chunjing Xu, Chao Xu, and Wen Gao. Pre-trained image processing transformer. In *Proceedings of the IEEE/CVF Conference on Computer Vision and Pattern Recognition (CVPR)*, 2021.
- [10] Mark Chen, Alec Radford, Rewon Child, Jeffrey Wu, Heewoo Jun, David Luan, and Ilya Sutskever. Generative pretraining from pixels. In *International Conference on Machine Learning (ICML)*, 2020.
- [11] Xiangxiang Chu, Zhi Tian, Bo Zhang, Xinlong Wang, Xiaolin Wei, Huaxia Xia, and Chunhua Shen. Conditional positional encodings for vision transformers. *arXiv preprint arXiv:2102.10882*, 2021.
- [12] Jieren Deng, Yijue Wang, Ji Li, Chenghong Wang, Chao Shang, Hang Liu, Sanguthevar Rajasekaran, and Caiwen Ding. Tag: Gradient attack on transformer-based language models. In *Findings of the Association for Computational Linguistics: EMNLP*, 2021.

- [13] Jacob Devlin, Ming-Wei Chang, Kenton Lee, and Kristina Toutanova. Bert: Pre-training of deep bidirectional transformers for language understanding. In *Annual Conference of the North American Chapter of the Association for Computational Linguistics (NAACL)*, 2018.
- [14] Alexey Dosovitskiy, Lucas Beyer, Alexander Kolesnikov, Dirk Weissenborn, Xiaohua Zhai, Thomas Unterthiner, Mostafa Dehghani, Matthias Minderer, Georg Heigold, Sylvain Gelly, et al. An image is worth 16x16 words: Transformers for image recognition at scale. In *International Conference on Learning Representations (ICLR)*, 2020.
- [15] Lixin Fan, Kam Woh Ng, Ce Ju, Tianyu Zhang, Chang Liu, Chee Seng Chan, and Qiang Yang. Rethinking privacy preserving deep learning: How to evaluate and thwart privacy attacks. In *Federated Learning*, pages 32–50. 2020.
- [16] Jonas Gehring, Michael Auli, David Grangier, Denis Yarats, and Yann N Dauphin. Convolutional sequence to sequence learning. In *International Conference on Machine Learning (ICML)*, 2017.
- [17] Jonas Geiping, Hartmut Bauermeister, Hannah Dröge, and Michael Moeller. Inverting gradients-how easy is it to break privacy in federated learning? *Advances in Neural Information Processing Systems (NeurIPS)*, 2020.
- [18] Kai Han, Yunhe Wang, Hanting Chen, Xinghao Chen, Jianyuan Guo, Zhenhua Liu, Yehui Tang, An Xiao, Chunjing Xu, Yixing Xu, et al. A survey on visual transformer. *arXiv*, 2020.
- [19] Ali Hatamizadeh, Hongxu Yin, Holger Roth, Wenqi Li, Jan Kautz, Daguang Xu, and Pavlo Molchanov. Gradvit: Gradient inversion of vision transformers. In *Proceedings of the IEEE/CVF Conference on Computer Vision and Pattern Recognition (CVPR)*, 2022.
- [20] Kaiming He, Xinlei Chen, Saining Xie, Yanghao Li, Piotr Dollár, and Ross Girshick. Masked autoencoders are scalable vision learners. In *Proceedings of the IEEE/CVF Conference on Computer Vision and Pattern Recognition (CVPR)*, 2022.
- [21] Kaiming He, Xiangyu Zhang, Shaoqing Ren, and Jian Sun. Deep residual learning for image recognition. In *Proceedings of the IEEE/CVF Conference on Computer Vision and Pattern Recognition (CVPR)*, 2016.
- [22] Shuting He, Hao Luo, Pichao Wang, Fan Wang, Hao Li, and Wei Jiang. Transreid: Transformer-based object re-identification. In *Proceedings of the IEEE/CVF International Conference on Computer Vision (ICCV)*, 2021.
- [23] Dan Hendrycks and Thomas Dietterich. Benchmarking neural network robustness to common corruptions and perturbations. *arXiv preprint arXiv:1903.12261*, 2019.
- [24] Dan Hendrycks, Kevin Zhao, Steven Basart, Jacob Steinhardt, and Dawn Song. Natural adversarial examples. *Proceedings of the IEEE/CVF Conference on Computer Vision and Pattern Recognition (CVPR)*, 2021.
- [25] Elad Hoffer, Tal Ben-Nun, Itay Hubara, Niv Giladi, Torsten Hoefer, and Daniel Soudry. Augment your batch: Improving generalization through instance repetition. In *Proceedings of the IEEE/CVF Conference on Computer Vision and Pattern Recognition (CVPR)*, 2020.
- [26] Jinwoo Jeon, Kangwook Lee, Sewoong Oh, Jungseul Ok, et al. Gradient inversion with generative image prior. *Advances in Neural Information Processing Systems (NeurIPS)*, 2021.
- [27] Yifan Jiang, Shiyu Chang, and Zhangyang Wang. Transgan: Two pure transformers can make one strong gan, and that can scale up. *Advances in Neural Information Processing Systems (NeurIPS)*, 2021.
- [28] Yunjae Jung, Donghyeon Cho, Sanghyun Woo, and In So Kweon. Global-and-local relative position embedding for unsupervised video summarization. In *European Conference on Computer Vision (ECCV)*, 2020.
- [29] Salman Khan, Muzammal Naseer, Munawar Hayat, Syed Waqas Zamir, Fahad Shahbaz Khan, and Mubarak Shah. Transformers in vision: A survey. *ACM Computing Surveys*, 2021.
- [30] Diederik P Kingma and Jimmy Ba. Adam: A method for stochastic optimization. In *International Conference on Learning Representations (ICLR)*, 2015.
- [31] Shun Kiyono, Sosuke Kobayashi, Jun Suzuki, and Kentaro Inui. Shape: Shifted absolute position embedding for transformers. *arXiv preprint arXiv:2109.05644*, 2021.

- [32] Jakub Konečný, Brendan McMahan, and Daniel Ramage. Federated optimization: Distributed optimization beyond the datacenter. *arXiv preprint arXiv:1511.03575*, 2015.
- [33] Jingyun Liang, Jiezhong Cao, Guolei Sun, Kai Zhang, Luc Van Gool, and Radu Timofte. Swinir: Image restoration using swin transformer. In *Proceedings of the IEEE/CVF International Conference on Computer Vision (ICCV)*, 2021.
- [34] Yahui Liu, Enver Sangineto, Wei Bi, Nicu Sebe, Bruno Lepri, and Marco Nadai. Efficient training of visual transformers with small datasets. *Advances in Neural Information Processing Systems (NeurIPS)*, 2021.
- [35] Yingfei Liu, Tiancai Wang, Xiangyu Zhang, and Jian Sun. Petr: Position embedding transformation for multi-view 3d object detection. *arXiv preprint arXiv:2203.05625*, 2022.
- [36] Yinhan Liu, Myle Ott, Naman Goyal, Jingfei Du, Mandar Joshi, Danqi Chen, Omer Levy, Mike Lewis, Luke Zettlemoyer, and Veselin Stoyanov. Roberta: A robustly optimized bert pretraining approach. *arXiv preprint arXiv:1907.11692*, 2019.
- [37] Ze Liu, Yutong Lin, Yue Cao, Han Hu, Yixuan Wei, Zheng Zhang, Stephen Lin, and Baining Guo. Swin transformer: Hierarchical vision transformer using shifted windows. In *Proceedings of the IEEE/CVF International Conference on Computer Vision (ICCV)*, 2021.
- [38] Jiahao Lu, Xi Sheryl Zhang, Tianli Zhao, Xiangyu He, and Jian Cheng. April: Finding the achilles’ heel on privacy for vision transformers. In *AAAI Workshop on Privacy-Preserving Artificial Intelligence*, 2021.
- [39] Leland McInnes, John Healy, and James Melville. Umap: Uniform manifold approximation and projection for dimension reduction. *arXiv preprint arXiv:1802.03426*, 2018.
- [40] Xudong Pan, Mi Zhang, Yifan Yan, Jiaming Zhu, and Min Yang. Theory-oriented deep leakage from gradients via linear equation solver. *arXiv preprint arXiv:2010.13356*, 2020.
- [41] Le Trieu Phong, Yoshinori Aono, Takuya Hayashi, Lihua Wang, and Shiho Moriai. Privacy-preserving deep learning: Revisited and enhanced. In *International Conference on Applications and Techniques in Information Security*, 2017.
- [42] Jia Qian, Hiba Nassar, and Lars Kai Hansen. Minimal conditions analysis of gradient-based reconstruction in federated learning. *arXiv preprint arXiv:2010.15718*, 2020.
- [43] Olga Russakovsky, Jia Deng, Hao Su, Jonathan Krause, Sanjeev Satheesh, Sean Ma, Zhiheng Huang, Andrej Karpathy, Aditya Khosla, Michael Bernstein, et al. Imagenet large scale visual recognition challenge. *International Journal of Computer Vision*, 115(3):211–252, 2015.
- [44] Peter Shaw, Jakob Uszkoreit, and Ashish Vaswani. Self-attention with relative position representations. In *Proceedings of the Conference of the North American Chapter of the Association for Computational Linguistics (NAACL)*, 2018.
- [45] Reza Shokri and Vitaly Shmatikov. Privacy-preserving deep learning. In *Proceedings of the ACM SIGSAC Conference on Computer and Communications Security*, 2015.
- [46] Jianlin Su, Yu Lu, Shengfeng Pan, Bo Wen, and Yunfeng Liu. Roformer: Enhanced transformer with rotary position embedding. *arXiv preprint arXiv:2104.09864*, 2021.
- [47] Ilya O Tolstikhin, Neil Houlsby, Alexander Kolesnikov, Lucas Beyer, Xiaohua Zhai, Thomas Unterthiner, Jessica Yung, Andreas Steiner, Daniel Keysers, Jakob Uszkoreit, et al. Mlp-mixer: An all-mlp architecture for vision. *Advances in Neural Information Processing Systems (NeurIPS)*, 2021.
- [48] Hugo Touvron, Matthieu Cord, Matthijs Douze, Francisco Massa, Alexandre Sablayrolles, and Herve Jegou. Training data-efficient image transformers & distillation through attention. In *International Conference on Machine Learning (ICML)*, 2021.
- [49] Ashish Vaswani, Noam Shazeer, Niki Parmar, Jakob Uszkoreit, Llion Jones, Aidan N Gomez, Łukasz Kaiser, and Illia Polosukhin. Attention is all you need. In *Advances in Neural Information Processing Systems (NeurIPS)*, 2017.
- [50] Michael Veale, Reuben Binns, and Lilian Edwards. Algorithms that remember: model inversion attacks and data protection law. *Philosophical Transactions of the Royal Society A: Mathematical, Physical and Engineering Sciences*, 376(2133):20180083, 2018.

- [51] Thijs Vogels, Sai Praneeth Karimireddy, and Martin Jaggi. Powersgd: Practical low-rank gradient compression for distributed optimization. In *Advances in Neural Information Processing Systems (NeurIPS)*, 2019.
- [52] Aidmar Wainakh, Fabrizio Ventola, Till Müßig, Jens Keim, Carlos Garcia Cordero, Ephraim Zimmer, Tim Grube, Kristian Kersting, and Max Mühlhäuser. User label leakage from gradients in federated learning. *arXiv preprint arXiv:2105.09369*, 2021.
- [53] Yangtao Wang, Xi Shen, Shell Xu Hu, Yuan Yuan, James L. Crowley, and Dominique Vaufreydaz. Self-supervised transformers for unsupervised object discovery using normalized cut. In *Proceedings of the IEEE/CVF Conference on Computer Vision and Pattern Recognition (CVPR)*, 2022.
- [54] Yu-An Wang and Yun-Nung Chen. What do position embeddings learn? an empirical study of pre-trained language model positional encoding. In *Proceedings of the Conference on Empirical Methods in Natural Language Processing (EMNLP)*, 2020.
- [55] Yuqing Wang, Zhaoliang Xu, Xinlong Wang, Chunhua Shen, Baoshan Cheng, Hao Shen, and Huaxia Xia. End-to-end video instance segmentation with transformers. In *Proceedings of the IEEE/CVF Conference on Computer Vision and Pattern Recognition (CVPR)*, 2021.
- [56] Zhibo Wang, Mengkai Song, Zhifei Zhang, Yang Song, Qian Wang, and Hairong Qi. Beyond inferring class representatives: User-level privacy leakage from federated learning. In *IEEE International Conference on Computer Communications*, 2019.
- [57] Chen Wei, Haoqi Fan, Saining Xie, Chao-Yuan Wu, Alan Yuille, and Christoph Feichtenhofer. Masked feature prediction for self-supervised visual pre-training. *arXiv preprint arXiv:2112.09133*, 2021.
- [58] Zhenda Xie, Zheng Zhang, Yue Cao, Yutong Lin, Jianmin Bao, Zhuliang Yao, Qi Dai, and Han Hu. Simmim: A simple framework for masked image modeling. *arXiv preprint arXiv:2111.09886*, 2021.
- [59] Guanglei Yang, Hao Tang, Mingli Ding, Nicu Sebe, and Elisa Ricci. Transformer-based attention networks for continuous pixel-wise prediction. In *Proceedings of the IEEE/CVF International Conference on Computer Vision (ICCV)*, 2021.
- [60] Hongxu Yin, Arun Mallya, Arash Vahdat, Jose M Alvarez, Jan Kautz, and Pavlo Molchanov. See through gradients: Image batch recovery via gradinversion. In *Proceedings of the IEEE/CVF Conference on Computer Vision and Pattern Recognition (CVPR)*, 2021.
- [61] Hongxu Yin, Pavlo Molchanov, Jose M Alvarez, Zhizhong Li, Arun Mallya, Derek Hoiem, Niraj K Jha, and Jan Kautz. Dreaming to distill: Data-free knowledge transfer via deepinversion. In *Proceedings of the IEEE/CVF Conference on Computer Vision and Pattern Recognition (CVPR)*, 2020.
- [62] Sangdoon Yun, Dongyoon Han, Seong Joon Oh, Sanghyuk Chun, Junsuk Choe, and Youngjoon Yoo. Cutmix: Regularization strategy to train strong classifiers with localizable features. In *Proceedings of the IEEE/CVF International Conference on Computer Vision (ICCV)*, 2019.
- [63] Hongyi Zhang, Moustapha Cisse, Yann N Dauphin, and David Lopez-Paz. mixup: Beyond empirical risk minimization. In *International Conference on Learning Representations (ICLR)*, 2018.
- [64] Richard Zhang, Phillip Isola, Alexei A Efros, Eli Shechtman, and Oliver Wang. The unreasonable effectiveness of deep features as a perceptual metric. In *Proceedings of the IEEE/CVF Conference on Computer Vision and Pattern Recognition (CVPR)*, 2018.
- [65] Bo Zhao, Konda Reddy Mopuri, and Hakan Bilen. idlg: Improved deep leakage from gradients. *arXiv preprint arXiv:2001.02610*, 2020.
- [66] Sixiao Zheng, Jiachen Lu, Hengshuang Zhao, Xiatian Zhu, Zekun Luo, Yabiao Wang, Yanwei Fu, Jianfeng Feng, Tao Xiang, Philip HS Torr, et al. Rethinking semantic segmentation from a sequence-to-sequence perspective with transformers. In *Proceedings of the IEEE/CVF Conference on Computer Vision and Pattern Recognition (CVPR)*, 2021.
- [67] Junyi Zhu and Matthew Blaschko. R-gap: Recursive gradient attack on privacy. In *International Conference on Learning Representations (ICLR)*, 2021.
- [68] Ligeng Zhu, Zhijian Liu, and Song Han. Deep leakage from gradients. In *Advances in Neural Information Processing Systems (NeurIPS)*, 2019.

[69] Xizhou Zhu, Weijie Su, Lewei Lu, Bin Li, Xiaogang Wang, and Jifeng Dai. Deformable detr: Deformable transformers for end-to-end object detection. In *International Conference on Learning Representations (ICLR)*, 2021.

A Training Setting

In the experiments on ImageNet-1K, we employ an AdamW [30] optimizer for 300 epochs using a cosine decay learning rate scheduler and 20 epochs of linear warm-up. A batch size of 1024, an initial learning rate of 0.001, and a weight decay of 0.05 are used. We include most of the augmentation and regularization strategies (e.g., repeated augmentation [25], CutMix [62], and Mixup [63]) of [48] in training, as shown in Table 6.

Table 6: Ingredients and hyper-parameters for our method.

| | |
|----------------------------|--|
| Epochs | 300 |
| Batch size | 1024 |
| Optimizer | AdamW |
| learning rate | $0.0005 \times \frac{\text{batchsize}}{512}$ |
| Learning rate decay | cosine |
| Weight decay | 0.05 |
| Warmup epochs | 20 |
| Label smoothing ϵ | 0.1 |
| Dropout | × |
| Repeated Aug | ✓ |
| Gradient Clip. | ✓ |
| Rand Augment | 9/0.5 |
| Mixup prob. | 0.8 |
| Cutmix prob. | 1.0 |
| Erasing prob. | 0.25 |

B Training Efficiency

We train our proposed method on ImageNet-1K with 8 V100 NVIDIA GPUs. We note that the computational consumption of the MJP procedure is negligible (*i.e.*, +2% time consumption per epoch). Meanwhile, MJP accelerates the convergence during the training as show in Figure 6.

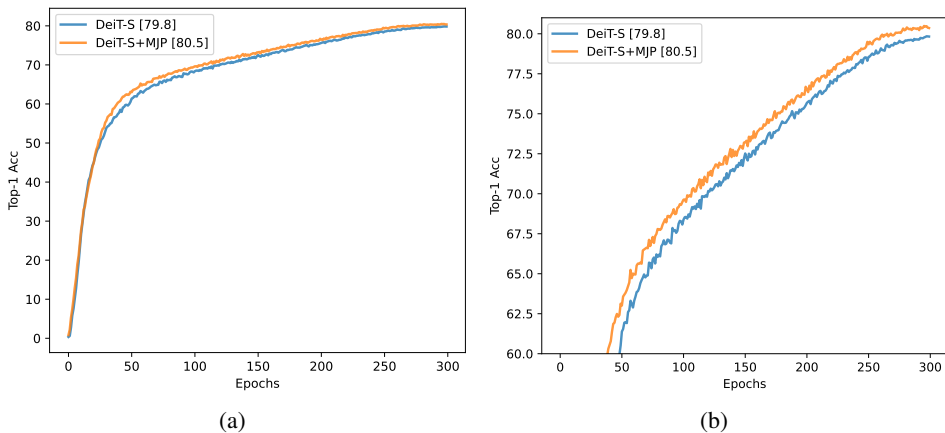


Figure 6: Comparisons the top-1 accuracy of DeiT-S and DeiT-S+MJP during the training: (a) the whole training and (b) a zoom-in screenshot for the accuracy larger than 60%.

C Position Embeddings

PCA Projected Dimensionality. Table 7 presents the explained variance (EV) of our DeiT-S+MJP and DeiT-S versus different projection dimension. A low dimensionality can explain a large amount of information, which proves that the embedding matrix is sparse in nature. Moreover, to achieve the same explained variance ratio, our DeiT-S+MJP needs a large dimensional than DeiT-S. This indicates that the positional embedding matrix of DeiT-S+MJP is less sparse and more informative.

Table 7: Explained variance versus PCA projected dimensionality.

| Projected Dimension | 3 | 4 | 5 | 6 | 7 |
|---------------------|-------|-------|-------|-------|-------|
| DeiT-S EV (%) | 54.61 | 68.55 | 77.95 | 85.54 | 90.74 |
| DeiT-S+MJP EV (%) | 46.74 | 58.36 | 69.10 | 78.13 | 84.55 |

Position Regression. Inspired by Wang *et al.* [54], we also check whether a position embedding can actually capture its absolute position. To some extent, such position information could be reconstructed by a reversed mapping function $g : \mathcal{X} \rightarrow \mathcal{P}$, where \mathcal{X} and \mathcal{P} are embedding space and position space, respectively. Thus, we use linear regression to learn such a function g that transfers the embeddings to the original positions. For the position embeddings in ViTs, we can map them into either 1-D sequence space or 2-D patch grid space. Given we only have 196 data points (*i.e.*, 224×224 image resolution with 16×16 patch size) for each learned embedding, a 5-fold cross-validation is applied to avoid overfitting. The reversed mapping functions are evaluated by Mean Absolute Error (MAE), and the result is shown in Table 8.

Table 8: Mean absolute error of the reversed mapping function learned by linear regression.

| Method | 1D MAE | 2D MAE |
|--------------------------|------------|-----------|
| DeiT-S [48] | .945±.031 | .076±.004 |
| DeiT-S + MJP (DAL - LN) | .566±.013 | .042±.002 |
| DeiT-S + MJP (DAL - NLN) | 1.301±.035 | .134±.003 |

From the results, the reversed mapping function of learnt position embeddings by “DeiT-S + MJP (DAL-LN)” can better represent the absolute positions. Meanwhile, the embeddings learned by the original DeiT-S and “DeiT-S + MJP (DAL-NLN)” also well learn the information about the absolute positions. Similar to [54], we have also tried some more complicated non-linear models such as SVM or MLP to map the embeddings back, which suffer from overfitting issue and perform worse. This implies that the position information in ViTs can actually be modeled by a linear model, which is consistent with Transformer encoders used in NLP field. Besides, the MAE of “DeiT-S+MJP (DAL - NLN)” is larger than the MAE of “DeiT-S+MJP (DAL - LN)” in Table 8. It indicates the nonlinear regression during the training aggregate more information beyond the position information (*i.e.*, more informative). The results are consistent with the Figure 3 (*i.e.*, accumulated top eigenvalues of position embeddings) in Section §5 in the main paper.

Projections of Position Embeddings. As shown in Figure 7, the position embeddings learned by the original DeiT-S is in a form of structured grids. Once we introduce MJP strategy to the training, it makes the projection of these position embeddings less structured. Meanwhile, the spatial-wise relative position information is preserved. We assume that the additional information (*i.e.*, more informative) in the position embeddings leads to such a difference.

D Robustness to Corruptions

We show the details on the evaluation with ImageNet-C [23], as shown in Table 9. Compared to the original DeiT-S, our method achieves better performance on most tested corruptions.

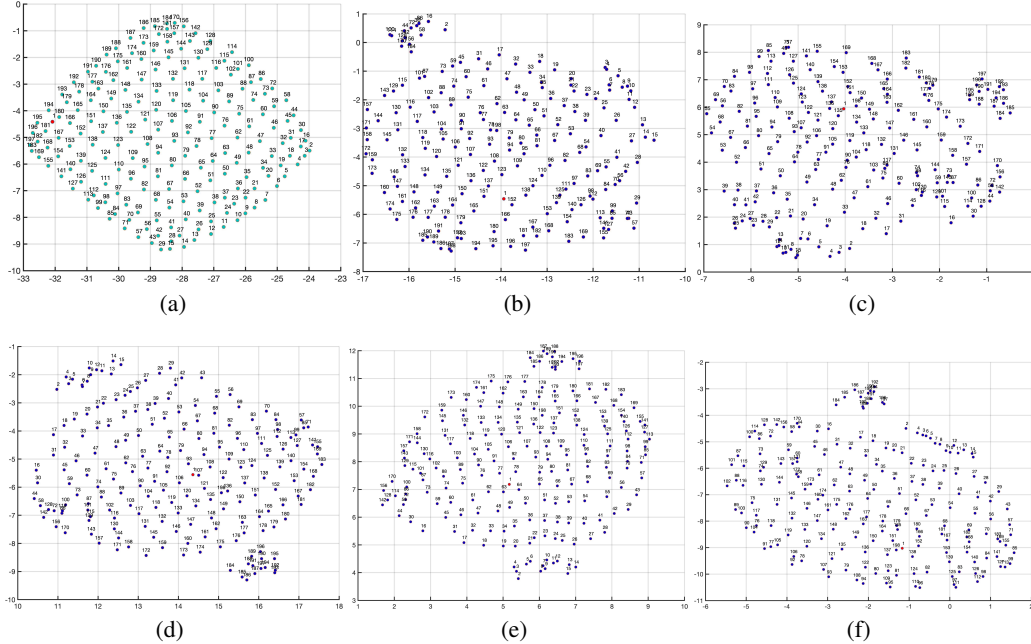


Figure 7: UMAP projections of the position embeddings collected from: (a) the original DeiT-S [14], (b) - (f) are DeiT-S+MJP trained with masking ratio $\gamma = \{0.1, 0.3, 0.5, 0.7, 0.9\}$ respectively.

Table 9: Comparisons on robustness to common corruptions with ImageNet-C.

| Method | Gaussian noise | Shot noise | Impulse noise | Defocus blur | Glass blur | Motion blur | Contrast | Elastic | Pixelate | JPEG | mCE \downarrow |
|--------------|----------------|-------------|---------------|--------------|-------------|-------------|-------------|-------------|-------------|-------------|------------------|
| DeiT-S | 41.0 | 42.7 | 42.8 | 50.5 | 59.4 | 45.5 | 36.1 | 43.0 | 42.4 | 36.6 | 44.0 |
| DeiT-S + MJP | 39.9 | 41.8 | 41.2 | 49.9 | 58.6 | 47.4 | 34.5 | 43.3 | 40.0 | 35.8 | 41.5 |

E More visual results

Figure 8 and Figure 9 shows more visual results on image recovery with the gradient updates. Obviously, our method alleviates the privacy leakage issue a lot compared to the baselines, where most of the details are lost in the reconstructed images.

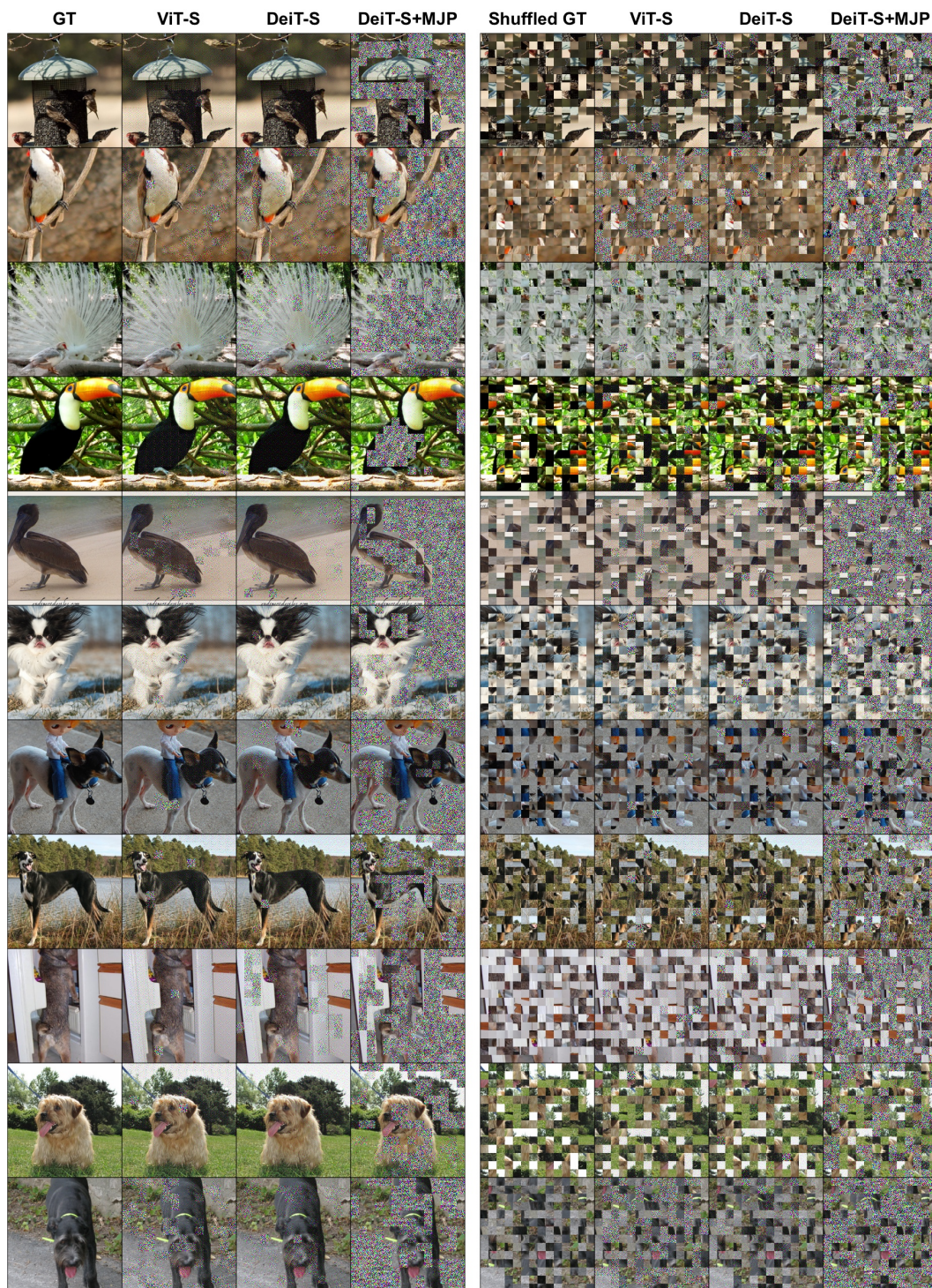


Figure 8: Visual comparisons on image recovery with gradient updates [38]. We test both the original images without shuffling the patches and images shuffled with a masked ratio $\gamma = 0.9$.

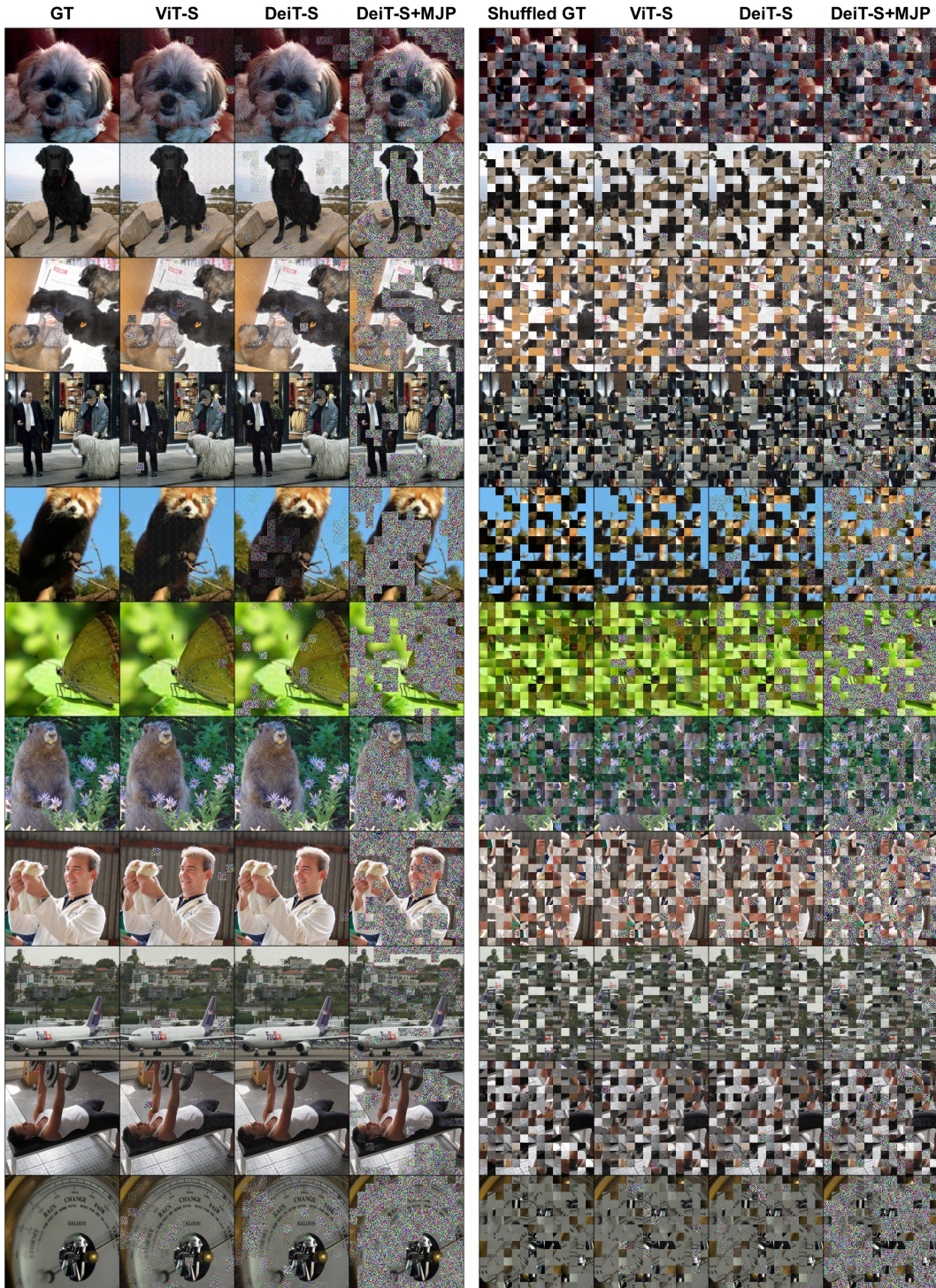


Figure 9: Visual comparisons on image recovery with gradient updates [38]. We test both the original images without shuffling the patches and images shuffled with a masked ratio $\gamma = 0.9$.